THE JOURNAL OF PHYSICAL CHEMISTRY C

Article

pubs.acs.org/JPCC

Anchoring Small Au Clusters on the Dehydroxylated and Hydroxylated SiO_2 α-Quartz (001) Surface via Ti-Alloying

Philomena Schlexer* and Gianfranco Pacchioni

Dipartimento di Scienza dei Materiali, Università Milano-Bicocca, via Cozzi 55, 20125 Milano, Italy

ABSTRACT: The adsorption of Au_xTi_y ($x + y = 4, 5$) bimetallic clusters on the hydroxyl-free and fully hydroxylated α-quartz (001) surfaces was investigated via density functional theory calculations including van der Waals (vdW) forces. The pure gold clusters adsorb only weakly on the silica surfaces via vdW forces. The interaction with the silica surfaces changes dramatically when Au atoms of the clusters are replaced by Ti. For $y \geq 2$, the clusters react with the surface via oxygen spillover (on the hydroxyl-free surface) and hydrogen spillover (on the hydroxylated surface). These bimetallic clusters with more than one Ti atom exhibit very large adsorption energies in the range of −3 to −9 eV. The substitution of only one Au atom by Ti ($y = 1$) results in an intermediate effect on the adsorption strength. It may, however, be sufficient for the in situ formation of gas-phase hydrogen via reaction of the clusters with surface hydroxyl groups, resulting in strongly bound $\equiv$Si−O−Au_xTi_y complexes.

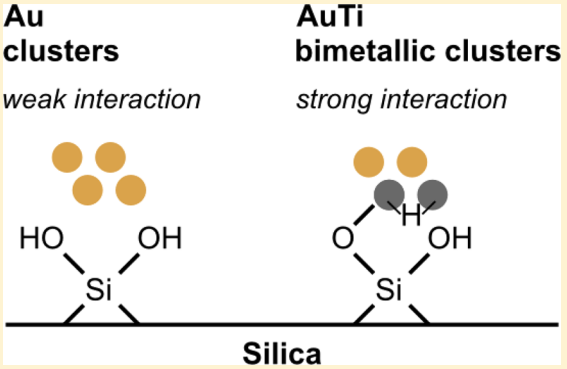

1. INTRODUCTION

Oxide-supported gold particles constitute active catalysts for a large variety of reactions, as, for instance, the CO oxidation reaction,[1−5] the water−gas shift reaction,[6−8] CO_2 hydrogenation,[9] and many more.[10,11] Also, subnanometer gold clusters were found to catalyze several reactions.[12,13] The reactivity of such oxide-supported metal clusters, consisting of only a few atoms, is an active research area.[14−16] The activity of oxide-supported Au clusters and nanoparticles is due to the finite size of the Au particles, as shown in the studies of Haruta et al. and similar works.[17,18] Therefore, morphological changes involving an increase in the mean particle size due to sintering is related to the loss of catalytic activity.[19−21] Au particles tend to sinter rapidly, even at room temperature; therefore, many strategies have been pursued to design sinter-resistant supported Au nanoparticles and clusters. For instance, the interaction of small Au clusters with oxides like SiO_2, TiO_2, or ZrO_2 can be increased significantly by introducing intrinsic and extrinsic defects on the oxide surface.[22−24] Also, small amounts of TiO_2 on SiO_2 and of SiO_2 on TiO_2 improved the stability of Au nanoparticles.[25,26]

Another strategy to combat the sintering of Au clusters is based on the modification of the Au clusters via alloying. Joshi et al. investigated the interaction of Au−Pd bimetallic clusters with the TS-1 zeolite and found no improvement of the cluster adsorption energy when Pd was introduced in the small Au clusters.[27] A more promising strategy is that to alloy the Au clusters with Ti. On the one hand, Bang et al. found that Au−Ti bimetallic clusters supported on TiO_2 show propitious properties for the CO oxidation reaction.[28] On the other hand, in larger Au−Ti bimetallic particles a possible oxidation of the Ti-part under reaction conditions leading to TiO_x units may presumably have promoting effects on the catalyst reactivity.[25] Furthermore, Toprek[29] and Dong[30] have shown with density functional theory (DFT) calculations that small Au−Ti bimetallic clusters exhibit a negative cohesion energy, indicating their intrinsic stability. Also, bulk Au−Ti binary alloys with different compositions have been synthesized.[31] Computational DFT-based alloy formation energies, taken from the online materials database aflowlib.org,[32] indicate that stable binary Au−Ti bulk alloys exist at different compositions. We checked all entries with the same computational setup and found stable alloys for all compositions with negative alloy formation energies according to $\Delta E_{form} = E(Au_x\ Ti_{1-x}) - x \cdot E(Au) - (1 - x) \cdot E(Ti)$, where $E(Au)$ and $E(Ti)$ are the total energies per atom of the elementary bulk materials.

In this study, we investigate how alloying subnanometer gold clusters with titanium, giving Au_xTi_y ($x + y = 4, 5$) bimetallic clusters, affects the cluster−support interaction with silica. With these calculations we want to simulate the preparation of model catalysts obtained by deposition of very small gas-phase metal clusters on silica under ultrahigh vacuum conditions (no reaction of the clusters with the surrounding environment). We chose silica as support, as here Au nanoparticles and clusters are known to be prone to sintering.[33] Furthermore, silica-supported Au particles have been shown to actively catalyze the CO oxidation reaction.[34] We represent the silica surface by a periodic slab model of the α-quartz (001) surface. To capture different features of silica surfaces, we considered the hydroxyl-free and the fully hydroxylated α-quartz (001) surfaces.

Received: May 9, 2017
Published: June 9, 2017

DOI: 10.1021/acs.jpcc.7b04420
J. Phys. Chem. C 2017, 121, 14717−14724

2. COMPUTATIONAL DETAILS

Periodic, spin-polarized DFT calculations were performed using the Vienna Ab Initio Simulation Package (VASP 5.2).[35−38] For the exchange-correlation functional, generalized gradient approximations (GGAs) were applied within the Perdew, Burke, and Ernzerhof (PBE) formulation.[39,40] To describe electron−ion interactions, the projector augmented wave (PAW) method was used.[41,42] O(2s, 2p), Si(3s, 3p), Au(5d, 6s), and Ti(3d, 4p, 4s) states are treated explicitly. The blocked Davidson iteration scheme was used for electronic relaxations.[43,44] In geometric structure optimizations, all ions were allowed to relax until ionic forces were <|0.01| eV/Å.

The slab models used to represent the hydroxyl-free and hydroxylated α-quartz (001) surfaces were described in our previous study.[45] A (2 × 2) surface super cell was used with lattice parameters of $a = b = 10.07$ Å and $\gamma = 60°$ and with a slab thickness of nine layers of $[SiO_4]$ tetrahedra. The slabs were separated by >15 Å of vacuum. Wave functions were expanded in the plane-wave basis up to a kinetic energy of 400 eV. A Γ-centered K-point grid in the Monkhorst−Pack scheme[46] was used, which was set to Γ-point for structure relaxations and to (3 × 3 × 1) for the DOS calculations. The structures, adsorption energies, and Bader charges do not change significantly when increasing the K-points to (3 × 3 × 1) for the structure optimizations. All atomic positions were allowed to change, and the lattice parameters were kept fixed during structure optimizations.

For the interaction between the metal clusters and the silica surface, vdW forces can be important.[47,48] Therefore, we used the semiempirical dispersion correction as proposed by Grimme,[49] known as the DFT-D2 approach, to investigate the adsorption of the clusters on the surface of the silica slabs. It is generally assumed that the DFT-D2 method can result in an overestimate of the dispersion interactions in certain systems, such as oxides. Therefore, we changed the parameters C_6 and R_0 of the DFT-D2 approach, as suggested by Tosoni and Sauer.[50] This method is denoted DFT-D2′ and is used for all of the calculations in this study. The DFT-D2′ method was found to reproduce well the results of higher level methods, as the vdW density functional designed by Lundqvist et al.,[51] for metal atoms and small clusters on oxides.[52,53] Atomic charges q were estimated via the Bader decomposition scheme.[54−56] The cohesive energies of the gas-phase clusters with respect to the gas-phase atoms were calculated as defined in eq 1.

$$E_{COH}(Au_xTi_y) = E(Au_xTi_y) - x\cdot E(Au) - y\cdot E(Ti) \quad (1)$$

Adsorption energies, E_{ADS}, were calculated as defined in eq 2, where $E(Au_xTi_y)$ are the metal clusters in the gas phase and S is the support.

$$E_{ADS}(Au_xTi_y/S) = E(Au_xTi_y/S) - E(Au_xTi_y) - E(S) \quad (2)$$

The support can either be the reconstructed hydroxyl-free α-quartz (001) surface S_R, the fully hydroxylated surface S_H, or the fully hydroxylated surface with a nonbridging oxygen S_{NBO} defect. All systems are structurally fully optimized.

When the metal clusters adsorb on the fully hydroxylated quartz surface, there is the possibility that they react with surface hydroxyl groups to form H_2 according to the following reaction, eq 3.

$$\equiv Si-OH + Au_xTi_y \rightarrow \frac{1}{2}H_2 + \equiv Si-O-Au_xTi_y \quad (3)$$

Here $\equiv Si-OH + Au_xTi_y$ corresponds to Au_xTi_y/S_H and $\equiv Si-O-Au_xTi_y$ corresponds to Au_xTi_y/S_{NBO}. Therefore, the corresponding reaction energy is given in eq 4, where $E(H_2)$ is the total energy of the gas-phase H_2 molecule.

$$E_{REA} = E(Au_xTi_y/S_{NBO}) + \frac{1}{2}E(H_2) - E(Au_xTi_y/S_H) \quad (4)$$

3. RESULTS

3.1. Gas-Phase Clusters. We optimized the structure of the gas-phase Au_xTi_y ($x + y = 4, 5$) bimetallic clusters considering various different structures (from 1D to 3D). Our results reproduce those of Dong et al.[30] We report the data for the gas-phase clusters here to compare them with the corresponding supported clusters. The cohesive energies per atom, Bader charges on Au atoms, and magnetic moments of the most stable results are summarized in Table 1. The cohesive energy per atom gradually increases with increasing Ti content. In the bimetallic gas-phase clusters, the Au atoms become negatively charged because of a charge transfer from Ti to Au. This is reflected in the Bader charges in Table 1. Many of the clusters have a nonzero magnetic moment. The spin density is in these cases mainly located on the 3d orbitals of the Ti atoms.

Table 1. Cohesive Energies Per Atom of Bimetallic Clusters $E_{COH}(Au_xTi_y)$ (eV), Sum of Bader Charges on the Au Atoms Σq (Au) (|e|), and Magnetic Moments on the Clusters μ (μ_B)

	$E_{COH}(Au_xTi_y)$	Σq(Au)	$\|\mu\|$
Au_4	−1.56	0.00	0.00
Au_3Ti	−2.43	−1.46	1.00
Au_2Ti_2	−2.45	−1.30	4.00
$AuTi_3$	−2.52	−0.86	5.00
Ti_4	−2.63		4.00
Au_5	−1.69	0.00	1.00
Au_4Ti	−2.27	−1.41	0.00
Au_3Ti_2	−2.68	−1.86	1.00
Au_2Ti_3	−2.69	−1.48	2.00
$AuTi_4$	−2.86	−0.73	5.00
Ti_5	−2.96		2.00

We considered all possible values for x and y in Au_xTi_y ($x + y = 4, 5$) for the gas-phase clusters. However, to study their adsorption on the silica surfaces, only a selection of clusters was considered (Figure 1). In all cases, the Ti atoms take a position in the center of the bimetallic clusters. Pure Au clusters and all bimetallic clusters prefer a planar geometry, whereas the pure Ti clusters show a 3D structure.

3.2. α-Quartz (001) Surface. Silica is a commonly used support material in catalysis because of its excellent chemical and thermal stability. There are various forms of silica available as catalyst support, whereby high-surface porous supports and sol−gel-derived forms are widely used because of their structural stabilization of the supported metal nanoparticles. To represent the silica support, we use the α-quartz modification of silica because of the possibility to represent it in a periodic super cell approach. α-Quartz is the thermodynamically most stable modification of silica under standard conditions, and the (001) surface is the most stable surface after surface reconstruction. To capture different

DOI: 10.1021/acs.jpcc.7b04420
J. Phys. Chem. C 2017, 121, 14717−14724

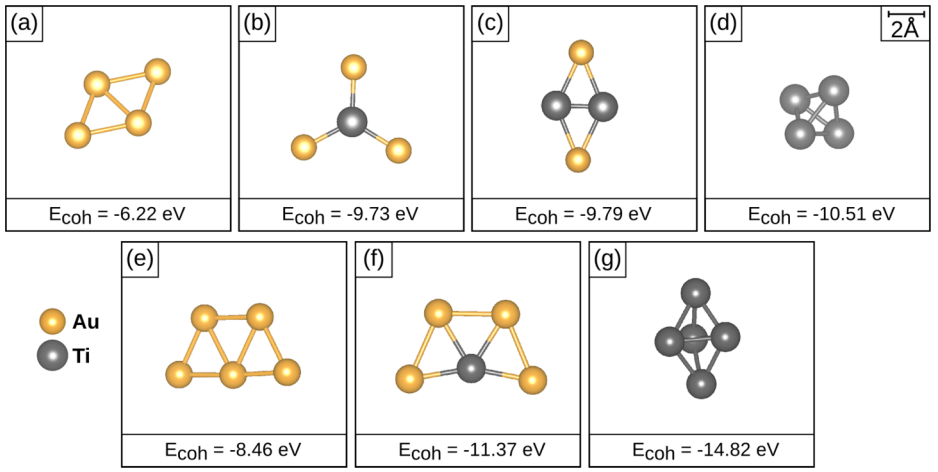

Figure 1. Optimal structures and cohesive energies, E_{COH} (eV), of Au_xTi_y gas-phase clusters. (a) Au_4, (b) Au_3Ti_1, (c) Au_2Ti_2, (d) Ti_4, (e) Au_5, (f) Au_4Ti_1, and (g) Ti_5.

chemical motifs present in the commonly used silica supports, we consider the hydroxyl-free (reconstructed) α-quartz (001) surface and the fully hydroxylated α-quartz (001) surface. The two surfaces are shown in Figure 2. The hydroxylated surface is formed by addition of water to the hydroxyl-free surface.

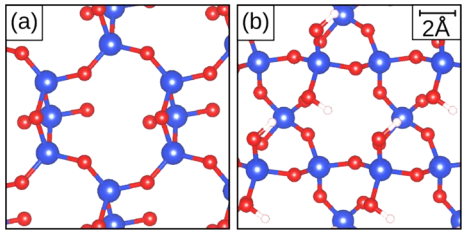

Figure 2. Top view of the α-quartz (001) surface. The first two layers of [SiO_2] units are shown. (a) Hydroxyl-free reconstructed surface and (b) fully hydroxylated surface.

3.3. Adsorption of the Clusters on the Hydroxyl-Free α-Quartz (001) Surface. The optimized gas-phase bimetallic clusters shown in Figure 1 were deposited on the hydroxyl-free α-quartz (001) surface. We investigated various adsorption configurations, but only the most stable cases are summarized in Table 2. The adsorption geometries are shown in Figure 3. The pure gold clusters adsorb only weakly via vdW-forces with adsorption energies of −0.21 eV for the Au tetramer and −0.26 eV for the Au pentamer. The ground-state nature of the cluster, closed or open shell, does not influence the adsorption mode. No charge transfer from the Au cluster to or from the support is observed, which is reflected in the Bader charges on the clusters close to 0 lel.

Table 2. Cluster Adsorption Energies $E_{ADS}(Au_xTi_y)$ (eV) on the Hydroxyl-Free α-Quartz (001) Surface, Sum of Bader Charges on the Au Atoms Σq(Au) [|el|], Sum of Bader Charges on the Ti Atoms Σq(Ti), Sum of Bader Charges on the Support $\Sigma q(SiO_2)$, and Total Moments on the Clusters μ (μ_B)

	$E_{ADS}(Au_xTi_y)$	Σq(Au)	Σq(Ti)	$\Sigma q(SiO_2)$	$\lvert\mu\rvert$
Au_4	−0.21	0.01		−0.01	0.00
Au_3Ti	−0.40	−1.49	1.55	−0.06	1.00
Au_2Ti_2	−3.30	−1.30	1.56	−0.26	0.00
Ti_4	−4.23		2.92	−2.92	2.00
Au_5	−0.26	0.03		−0.03	1.00
Au_4Ti	−0.57	−1.16	1.63	−0.47	1.98
Ti_5	−4.61		3.99	−3.99	0.00

Let us now consider the adsorption of the bimetallic clusters. The adsorption energies of clusters containing one Ti atom are slightly enhanced with respect to the pure gold clusters (Table 2). The geometry of the supported Au_3Ti cluster (Figure 3b) and that of the supported Au_4Ti cluster (Figure 3f) deviate from the perfectly planar structure in the gas-phase. This is because the Ti atoms are coordinated to surface oxygen atoms from the silica support. As for the gas-phase clusters, we observe a charge transfer from the Ti atoms to the Au atoms in the bimetallic clusters.

The adsorption energies of the bimetallic clusters are further enhanced for clusters containing more than one Ti atom (Table 2). For instance, the adsorption energy of the Au_2Ti_2 cluster is 2.9 eV more negative than that of Au_3Ti. The enhancement of the adsorption energy is related to the fact that the clusters react with the hydroxyl-free silica surface. Oxygen moves from the SiO_2 lattice and binds to the cluster (Figure 3c). This corresponds to an oxygen spillover from the oxide to the metal cluster, leading to a reduction of the support and the oxidation of the cluster. Clearly, this indicates that the Ti atoms of the cluster are intrinsically very reactive and, under real conditions, will react with any oxygen containing species present in the environment (O_2, water, etc.). The reduction of silica is reflected in the negative net charge on the support, which is represented by the sum of Bader charges on all Si and O atoms $\Sigma q(SiO_2)$. The charge transfer can also be seen in the DOS (Figure 4). For clusters containing more than one Ti atom, occupied Si 3s states can be detected (Figure 4c,d). The Si 3s states are hybridized with the Ti 3d states, indicating the formation of a polar-covalent bond. Furthermore, a hybridization between Ti 3d and O 2p states can be seen. Not surprisingly, the Ti clusters exhibit the largest adsorption energies and charge transfer (Table 2). Once more, Ti clusters are extremely reactive toward oxygen species and become oxidized at the expense of the silica surface.

3.4. Adsorption of the Clusters on the Hydroxylated α-Quartz (001) Surface. The optimized gas-phase clusters were deposited on the fully hydroxylated α-quartz (001)

DOI: 10.1021/acs.jpcc.7b04420
J. Phys. Chem. C 2017, 121, 14717−14724

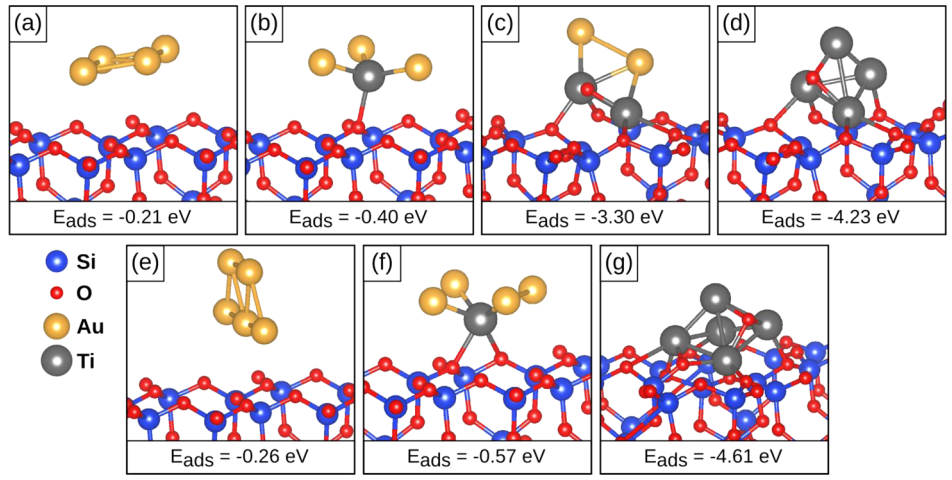

Figure 3. Optimal structures and adsorption energies E_{ADS} (eV) of Au_xTi_y clusters supported on the hydroxyl-free α-quartz (001) surface. (a) Au_4, (b) Au_3Ti_1, (c) Au_2Ti_2, (d) Ti_4, (e) Au_5, (f) Au_4Ti_1, and (g) Ti_5.

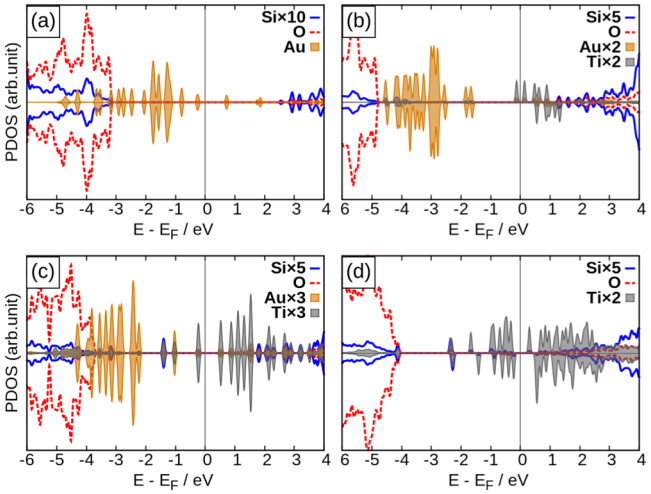

Figure 4. DOS curves of the Au_xTi_y clusters supported on the hydroxyl-free α-quartz (001) surface. (a) Au_4, (b) Au_3Ti_1, (c) Au_2Ti_2, and (d) Ti_4.

surface. Again, various adsorption positions and geometries were tested, but only the most stable configurations are discussed (Table 3). The adsorption energies of the clusters on the hydroxylated surface are significantly enhanced with respect to the hydroxyl-free surface (Table 2). In particular, the adsorption energies of the clusters containing one Ti atom are enhanced from roughly 0.5 eV on the hydroxyl-free surface to >1.5 eV on the hydroxylated surface. The hydroxyl groups stabilize the partial charges (negative on Au and positive on Ti) of the cluster via coordination with surface OH groups, resulting in a kind of solvation effect by oxygenated ligands. The Ti atoms are coordinated by oxygen atoms; furthermore, the hydrogen atoms point toward the Au atoms (Figure 5b,f).

The Ti_5 cluster constitutes a special case because it is so reactive that here we can observe the spontaneous formation of water (Figure 5g). Presumably, there are many more ways for the clusters to react with the surface. However, we did not investigate this aspect in detail because we are mainly interested in the trend of the adsorption strength of the bimetallic clusters. The formation of $TiO_{2(-x)}$ is certainly thermodynamically favorable compared with the pure Ti clusters.

As for the clusters supported on the hydroxyl-free surface, clusters with more than one Ti atom react with the silica surface, resulting in large adsorption energies (Table 3). However, this time we mainly observe hydrogen reverse spillover (Figure 5c,d,g). In this process, the hydroxyl groups are spontaneously split and the hydrogen atom binds onto the clusters having hydride character.[57] Recent studies show that this process is energetically favorable for late transition metal, except for Au.[58−60] The hydride character of the Ti−H bond is reflected in the occupied H 1s states (Figure 6c,d). Preliminary calculations on larger clusters (Au_{20} and $Au_{10}Ti_{10}$) supported on the fully hydroxylated surface confirm the observation made for the smaller clusters: Whereas the Au_{20} cluster adsorbs only weakly, the $Au_{10}Ti_{10}$ cluster reacts with the surface via hydrogen reverse spillover, resulting in a stronger binding of the cluster on the surface.

Table 3. Cluster Adsorption Energies $E_{ADS}(Au_xTi_y)$ (eV) on the Fully Hydroxylated α-Quartz (001) Surface[a]

	$E_{ADS}(Au_xTi_y)$	Σq(Au)	Σq(Ti)	$\Sigma q(SiO_2)$	$\lvert\mu\rvert$
Au_4	−0.88	−0.03		0.03	0.00
Au_3Ti	−1.63	−1.52	1.58	−0.06	1.00
Au_2Ti_2	−4.37	−1.30	2.58	−1.28	2.00
Ti_4	−7.25		2.86	−2.86	2.00
Au_5	−0.84	−0.01		0.01	1.00
Au_4Ti	−2.38	−1.66	1.72	−0.06	0.00
Ti_5	−6.62		1.97	−1.97	2.00

[a]Sum of Bader charges on the Au atoms Σq(Au) (|el|), sum of Bader charges on the Ti atoms Σq(Ti), sum of Bader charges on the support $\Sigma q(SiO_2)$, and magnetic moments on the clusters μ (μ_B).

3.5. Hydroxylated α-Quartz (001) Surface with Nonbridging Oxygen Defect. The nonbridging oxygen (NBO) defect is one of the most important intrinsic defects in silica. It is formally created via the removal of a neutral H atom from a hydroxyl group, leaving behind a paramagnetic ≡Si−O• unit. The presence of NBO defects on silica surfaces was proven experimentally via metastable impact electron spectroscopy (MIES) and ultraviolet photoelectron spectroscopy (UPS).[61,62] NBO defects quite remarkably influence the aggregation behavior of late transition-metal clusters and atoms supported on silica.[63,23] We therefore considered the effect of this defect on the adsorption mode of the bimetallic Au_xTi_y clusters. The

DOI: 10.1021/acs.jpcc.7b04420
J. Phys. Chem. C 2017, 121, 14717−14724

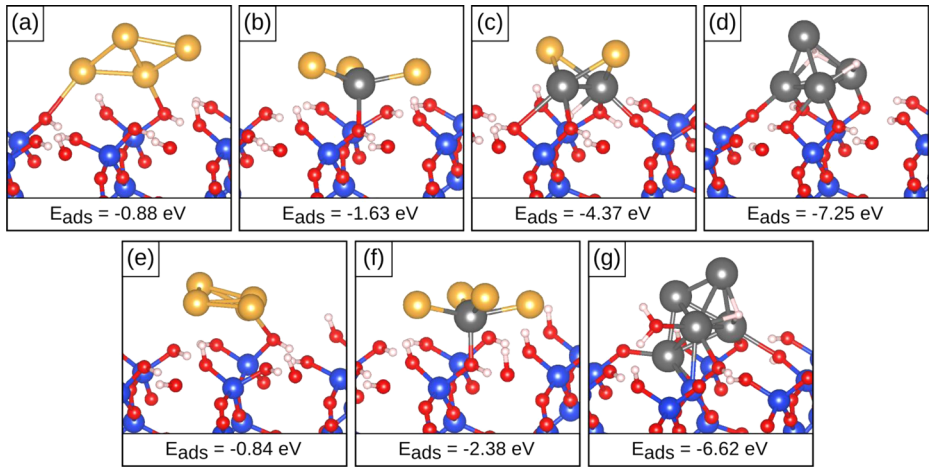

Figure 5. Optimal structures and adsorption energies E_{ADS} (eV) of Au_xTi_y clusters supported on the hydroxylated α-quartz (001) surface. (a) Au_4, (b) Au_3Ti_1, (c) Au_2Ti_2, (d) Ti_4, (e) Au_5, (f) Au_4Ti_1, and (g) Ti_5.

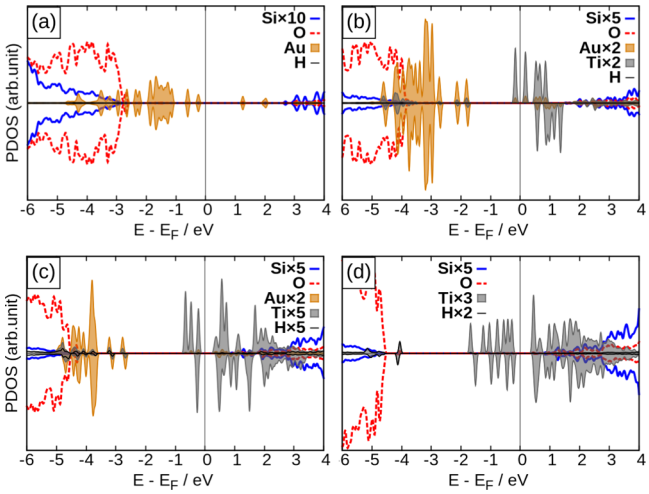

Figure 6. DOS curves of the Au_xTi_y clusters supported on the hydroxylated α-quartz (001) surface. (a) Au_4, (b) Au_3Ti_1, (c) Au_2Ti_2, and (d) Ti_4.

results are summarized in Table 4, and the adsorption geometries are shown in Figure 7.

The NBO defect has a substantial effect on the adsorption mode of the pure Au clusters, as similarly reported for Cu clusters.[64] For instance, the adsorption energy of the Au tetramer is enhanced by ~2.3 eV when going from the defect-free fully hydroxylated surface to the surface with a NBO defect. The presence of defects on the silica surface can therefore contribute to anchor pure Au clusters to the support. The Bader charge on the gold cluster is close to 0.5 |e|, suggesting a charge transfer from the cluster to the NBO center. Indeed, the paramagnetic O 2p state of the pristine ≡Si−O• unit cannot be observed in the DOS (Figure 8a). Instead, we detect an empty Au 6s state confirming the charge transfer (≡Si−O$^-$Au$^+$). Similar observations can also be made for the other clusters.

If one Au atom is substituted by Ti, then the clusters bind even more strongly to the surface. The Ti atoms are thereby directly bound to the unsaturated oxygen atom. Adsorption energies reach values of −6.13 for Au_3Ti and −5.96 for Au_4Ti. The net charge transfer from the clusters to the oxygen is reflected in the negative Bader charge on the support. For the clusters containing one Ti atom, the reaction for the formation of hydrogen is exothermic. This means that even clusters with quite low Ti content may be anchored to a hydroxylated silica surface because of the in situ formation of the ≡Si−O−Au_x Ti_y complex.

We have seen that the clusters with more than one Ti atom react with the defect-free, fully hydroxylated surface via hydrogen reverse spillover (Figure 5c,d). The adsorption of the clusters on a NBO defect can therefore be formally computed by desorbing one of the hydrogen atoms on the cluster. The resulting structures are shown in Figure 7c,d. The bonding of the hydrogen atoms on the Ti part of the clusters is quite strong, and so its desorption has a high energy cost. In fact, the reaction energy for the formation of the gas-phase hydrogen is endothermic for Au_2Ti_2 and Ti_4. So, clusters with higher Ti content do not tend to form gas-phase hydrogen. Instead, the hydrogen-reversed spillover is energetically more favorable.

Table 4. Cluster Adsorption Energies $E_{ADS}(Au_xTi_y)$ (eV), E_{REA} (eV), Sum of Bader Charges on the Au Atoms Σq(Au) (|e|), Sum of Bader Charges on Ti Atoms Σq(Ti), Sum of Bader Charges on the Support $\Sigma q(SiO_2)$, and Magnetic Moments on the Clusters μ (μ_B)

	$E_{ADS}(Au_xTi_y)$	E_{REA}	Σq(Au)	Σq(Ti)	$\Sigma q(SiO_2)$	$\lvert\mu\rvert$
Au_4	−3.17	0.93	0.49		−0.49	1.00
Au_3Ti	−6.13	−1.29	−1.29	1.87	−0.58	0.00
Au_2Ti_2	−6.88	0.71	−1.33	2.21	−0.88	3.00
Ti_4	−9.45	1.02		2.25	−2.25	1.00
Au_5	−3.35	0.70	0.47		−0.47	0.00
Au_4Ti	−5.96	−0.36	−1.18	1.75	−0.57	1.00
Ti_5	−8.55	1.29		2.30	−2.30	3.00

4. CONCLUSIONS

We investigated the adsorption of Au_xTi_y ($x + y = 4, 5$) bimetallic clusters on the reconstructed hydroxyl-free and the fully hydroxylated α-quartz (001) surfaces via DFT calculations including vdW forces. We find that on the hydroxyl-free silica surface gold clusters bind entirely via dispersion forces with quite small adsorption energies. This would imply high mobility and rapid sintering of the clusters at finite temperatures. Alloying the clusters with Ti significantly enhances the

DOI: 10.1021/acs.jpcc.7b04420
J. Phys. Chem. C 2017, 121, 14717−14724

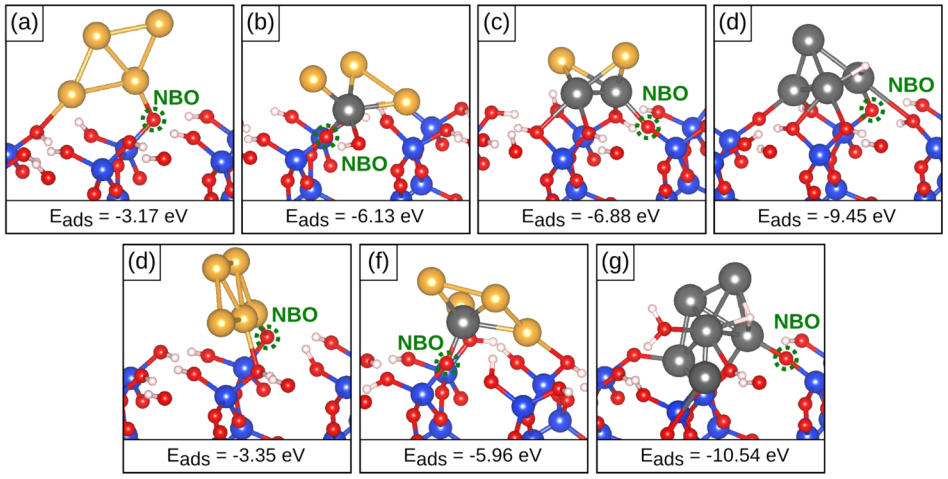

Figure 7. Optimal structures and adsorption energies E_{ADS} (eV) of Au_xTi_y clusters supported on the hydroxylated α-quartz (001) surface with a nonbridging oxygen (NBO) defect. (a) Au_4, (b) Au_3Ti_1, (c) Au_2Ti_2, (d) Ti_4, (e) Au_5, (f) Au_4Ti_1, and (g) Ti_5.

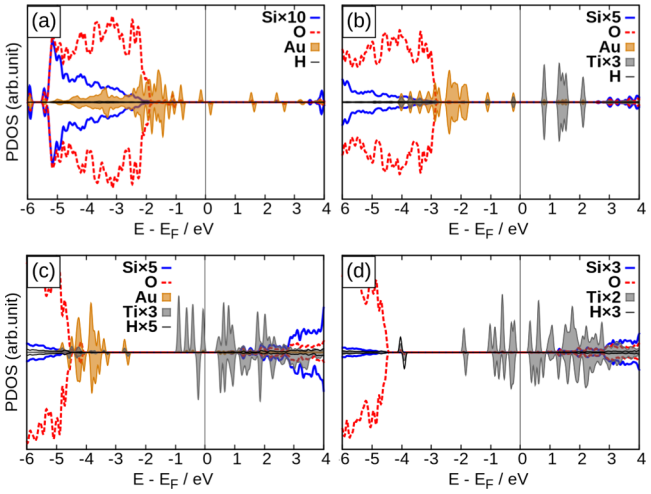

Figure 8. DOS curves of the Au_xTi_y clusters supported on the hydroxylated α-quartz (001) surface with a nonbridging oxygen (NBO) defect. (a) Au_4, (b) Au_3Ti_1, (c) Au_2Ti_2, and (d) Ti_4.

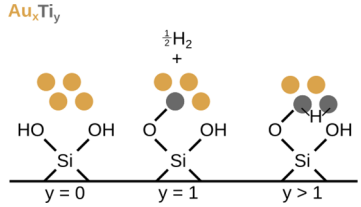

Figure 9. Schematic representation of the reactivity of Au_xTi_y ($x + y$ = 4, 5) bimetallic clusters supported on the fully hydroxylated α-quartz (001) surface. Whereas pure gold clusters (y = 0) interact only weakly with the silica surface, bimetallic clusters with one Ti atom (y = 1) react with the surface with the formation of 1/2 H_2. Bimetallic clusters with more than one Ti (y > 1) atom react with the surface under the formation of a hydride species adsorbed on the Ti component of the cluster.

adsorption energy, particularly for y > 1. Clusters with more than one Ti atom react with the hydroxyl-free silica surface via oxygen spillover, resulting in remarkably large adsorption energies in the range of −3.3 to −4.6 eV. In practice, the mixed Au−Ti cluster is oxidized at the expense of the silica surface, which is reduced (in this case by the formation of an oxygen vacancy). Under realistic conditions, the Ti component of the bimetallic cluster will become immediately oxidized with the formation of Au−TiO_x mixed clusters.

The situation is more complex on the fully hydroxylated surface because here essentially three cases become possible depending on the level of reactivity of the bimetallic cluster with the surface OH groups. This is schematically represented in Figure 9. A monometallic gold cluster interacts only weakly with the surface via van der Waals forces. In this respect there is little change compared with the hydroxyl-free surface. The substitution of one Au atom with Ti already results in a substantial enhancement of the adsorption energy, which is due to a "solvation" effect where the OH groups act as ligands. There is an internal charge transfer in the bimetallic cluster with the Au atoms becoming negatively charged at the expenses of the Ti component (positively charged). This offers the possibility to reinforce the interaction with the support via electrostatic bonding with the OH groups, which significantly stabilizes the supported cluster. Furthermore, the in situ formation of H_2 is also possible and is exothermic for clusters containing one Ti atom (Figure 9). This can effectively lead to their anchoring on the silica surface with adsorption energies of ∼6 eV. The favorable formation of gas-phase H_2 when a Au_xTi_y bimetallic cluster with low Ti content interacts with the surface OH groups is due to the low tendency of the cluster to bind the H atom after this has spilled over from the surface.

On the contrary, on clusters with more than one Ti atom, hydrogen reverse spillover is observed and results in very high adsorption energies of the bimetallic cluster to the surface, in the range of −4 to −7 eV. In this case, however, the in situ formation of H_2 is not thermodynamically favorable because the hydrogen atoms bind very strongly to the Ti part of the clusters forming a Ti−H−Ti hydride species. The desorption of H_2 into the gas phase is thus hindered (Figure 9).

These results show that the different composition of a bimetallic cluster composed of a very active metal (Ti) and a rather inert metal (Au) may result in a range of behaviors depending on the cluster composition. By changing the respective ratio of the two metals one can, in principle, modify the reactivity and the binding to the support in a desired way. These results have been obtained under the assumption that the cluster deposition occurs in ultrahigh vacuum so that the more reactive component of the metal cluster (Ti in this case)

DOI: 10.1021/acs.jpcc.7b04420
J. Phys. Chem. C 2017, 121, 14717−14724

arrives intact on the surface. Further work is needed to simulate AuTi bimetallic clusters in air because this implies a deep change of the cluster composition.

AUTHOR INFORMATION

Corresponding Author

*E-mail: philomena.schlexer@unimib.it.

ORCID

Philomena Schlexer: 0000-0002-3135-9089

Notes

The authors declare no competing financial interest.

ACKNOWLEDGMENTS

We thank Prof. Ib Chorkendorff, Bela Sebok, Prof. Richard Palmer, and Yubiao Niu for stimulating discussions. Financial support from the European Marie Curie Project CATSENSE (grant agreement number: 607417) is gratefully acknowledged.

REFERENCES

(1) Haruta, M.; Kobayashi, T.; Sano, H.; Yamada, N. Novel gold catalysts for the oxidation of carbon monoxide at a temperature far below 0°C. *Chem. Lett.* **1987**, *16*, 405−408.

(2) Haruta, M. Size- and support-dependency in the catalysis of gold. *Catal. Today* **1997**, *36*, 153−166.

(3) Li, L.; Gao, Y.; Li, H.; Zhao, Y.; Pei, Y.; Chen, Z.; Zeng, X. C. CO oxidation on TiO_2 (110) supported subnanometer gold clusters: size and shape effects. *J. Am. Chem. Soc.* **2013**, *135*, 19336−19346.

(4) Saavedra, J.; Doan, H. A.; Pursell, C. J.; Grabow, L. C.; Chandler, B. D. The critical role of water at the gold-titania interface in catalytic CO oxidation. *Science* **2014**, *345*, 1599−1602.

(5) Kim, H. Y.; Lee, H. M.; Henkelman, G. CO oxidation mechanism on CeO_2-supported Au nanoparticles. *J. Am. Chem. Soc.* **2012**, *134*, 1560−1570.

(6) Rodriguez, J. A.; Liu, P.; Hrbek, J.; Evans, J.; Pérez, M. Water gas shift reaction on Cu and Au nanoparticles supported on CeO_2(111) and ZnO(0001): Intrinsic activity and importance of support interactions. *Angew. Chem., Int. Ed.* **2007**, *46*, 1329−1332.

(7) Boccuzzi, F.; Chiorino, A.; Manzoli, M.; Andreeva, D.; Tabakova, T. FTIR study of the low-temperature water−gas shift reaction on Au/Fe_2O_3 and Au/TiO_2 catalysts. *J. Catal.* **1999**, *188*, 176−185.

(8) Williams, W. D.; Shekhar, M.; Lee, W. S.; Kispersky, V.; Delgass, W. N.; Ribeiro, F. H.; Kim, S. M.; Stach, E. A.; Miller, J. T.; Allard, L. F. J. Metallic corner atoms in gold clusters supported on rutile are the dominant active site during water− gas shift catalysis. *J. Am. Chem. Soc.* **2010**, *132*, 14018.

(9) Yang, X.; Kattel, S.; Senanayake, S. D.; Boscoboinik, J. A.; Nie, X.; Graciani, J.; Rodriguez, J. A.; Liu, P.; Stacchiola, D. J.; Chen, J. G. Low Pressure CO_2 hydrogenation to methanol over gold nanoparticles activated on a CeO_x/TiO_2 interface. *J. Am. Chem. Soc.* **2015**, *137*, 10104−10107.

(10) Corma, A.; Garcia, H. Supported gold nanoparticles as catalysts for organic reactions. *Chem. Soc. Rev.* **2008**, *37*, 2096−2126.

(11) Turner, M.; Golovko, V. B.; Vaughan, O. P.; Abdulkin, P.; Berenguer-Murcia, A.; Tikhov, M. S.; Johnson, B. F.; Lambert, R. M. Selective oxidation with dioxygen by gold nanoparticle catalysts derived from 55-atom clusters. *Nature* **2008**, *454*, 981−983.

(12) Liu, C.; Tan, Y.; Lin, S.; Li, H.; Wu, X.; Li, L.; Pei, Y.; Zeng, X. C. CO self-promoting oxidation on nanosized gold clusters: triangular Au_3 active site and CO induced O−O scission. *J. Am. Chem. Soc.* **2013**, *135*, 2583−2595.

(13) Yang, M.; Allard, L. F.; Flytzani-Stephanopoulos, M. Atomically dispersed Au-$(OH)_x$ species bound on titania catalyze the low-temperature water-gas shift reaction. *J. Am. Chem. Soc.* **2013**, *135*, 3768−3771.

(14) Liu, C.; Yang, B.; Tyo, E.; Seifert, S.; DeBartolo, J.; von Issendorff, B.; Zapol, P.; Vajda, S.; Curtiss, L. A. Carbon dioxide conversion to methanol over size-selected Cu_4 clusters at low pressures. *J. Am. Chem. Soc.* **2015**, *137*, 8676−8679.

(15) Heard, C. J.; Vajda, S.; Johnston, R. L. Support and Oxidation Effects on Subnanometer Palladium Nanoparticles. *J. Phys. Chem. C* **2014**, *118*, 3581−3589.

(16) Cheng, L.; Yin, C.; Mehmood, F.; Liu, B.; Greeley, J.; Lee, S.; Lee, B.; Seifert, S.; Winans, R. E.; Teschner, D.; et al. Reaction mechanism for direct propylene epoxidation by alumina-supported silver aggregates: the role of the particle/support interface. *ACS Catal.* **2014**, *4*, 32−39.

(17) Valden, M.; Lai, X.; Goodman, D. W. Onset of catalytic activity of gold clusters on titania with the appearance of nonmetallic properties. *Science* **1998**, *281*, 1647−1650.

(18) Boccuzzi, F.; Chiorino, A.; Manzoli, M.; Lu, P.; Akita, T.; Ichikawa, S.; Haruta, M. Au/TiO_2 nanosized samples: A catalytic, TEM, and FTIR study of the effect of calcination temperature on the CO oxidation. *J. Catal.* **2001**, *202*, 256−267.

(19) Denkwitz, Y.; Schumacher, B.; Kučerová, G.; Behm, R. J. Activity, stability, and deactivation behavior of supported Au/TiO_2 catalysts in the CO oxidation and preferential CO oxidation reaction at elevated temperatures. *J. Catal.* **2009**, *267*, 78−88.

(20) Chen, M. S.; Goodman, D. W. Structure−activity relationships in supported Au catalysts. *Catal. Today* **2006**, *111*, 22−33.

(21) Valden, M.; Pak, S.; Lai, X.; Goodman, D. W. Structure sensitivity of CO oxidation over model Au/TiO_2 catalysts. *Catal. Lett.* **1998**, *56*, 7−10.

(22) Schlexer, P.; Puigdollers, A. R.; Pacchioni, G. Tuning the charge state of Ag and Au atoms and clusters deposited on oxide surfaces by doping: a DFT study of the adsorption properties of nitrogen- and niobium-doped TiO_2 and ZrO_2. *Phys. Chem. Chem. Phys.* **2015**, *17*, 22342−22360.

(23) Schlexer, P.; Pacchioni, G. Adsorption and dimerization of late transition metal atoms on the regular and defective quartz (001) surface. *Top. Catal.* **2017**, *60*, 459.

(24) Gong, X. Q.; Selloni, A.; Dulub, O.; Jacobson, P.; Diebold, U. Small Au and Pt clusters at the anatase TiO_2 (101) surface: behavior at terraces, steps, and surface oxygen vacancies. *J. Am. Chem. Soc.* **2008**, *130*, 370−381.

(25) Gabaldon, J. P.; Bore, M.; Datye, A. K. Mesoporous silica supports for improved thermal stability in supported Au catalysts. *Top. Catal.* **2007**, *44*, 253−262.

(26) Rashkeev, S. N.; Dai, S.; Overbury, S. H. Modification of Au/TiO_2 Nanosystems by SiO_2 Monolayers: Toward the Control of the Catalyst Activity and Stability. *J. Phys. Chem. C* **2010**, *114*, 2996−3002.

(27) Joshi, A. M.; Delgass, W. N.; Thomson, K. T. Partial oxidation of propylene to propylene oxide over a neutral gold trimer in the gas phase: a density functional theory study. *J. Phys. Chem. B* **2006**, *110*, 2572−2581.

(28) Bang, K.; Shin, K.; Ryu, M. S.; Kwon, S.; Lee, H. M. Titanium-promoted Au-Ti bimetallic nanoparticle catalysts for CO oxidation: a theoretical approach. *Catal. Today* **2016**, *265*, 14−18.

(29) Toprek, D.; Koteski, V. Ab initio calculations of the structure, energetics and stability of Au_nTi (n = 1−32) clusters. *Comput. Theor. Chem.* **2016**, *1081*, 9−17.

(30) Dong, D.; Ben-Xia, Z.; Hui, W.; Quan, D. Geometries, stabilities, and magnetic properties of Au_nTi (n = 1−9) clusters: A density functional study. *Comput. Theor. Chem.* **2013**, *1025*, 67−73.

(31) Kikuchi, M.; Takahashi, M.; Okuno, O. Elastic moduli of cast Ti-Au, Ti-Ag, and Ti-Cu alloys. *Dent. Mater.* **2006**, *22*, 641−646.

(32) Curtarolo, S.; Setyawan, W.; Wang, S.; Xue, J.; Yang, K.; Taylor, R. H.; Nelson, L. J.; Hart, G. L.; Sanvito, S.; Buongiorno-Nardelli, M.; et al. AFLOWLIB.ORG: A distributed materials properties repository from high-throughput ab initio calculations. *Comput. Mater. Sci.* **2012**, *58*, 227−235.

(33) Min, B. K.; Wallace, W. T.; Goodman, D. W. Synthesis of a sinter-resistant, mixed-oxide support for Au nanoclusters. *J. Phys. Chem. B* **2004**, *108*, 14609−14615.

(34) Wu, Z.; Zhou, S.; Zhu, H.; Dai, S.; Overbury, S. H. DRIFTS-QMS study of room temperature CO oxidation on Au/SiO_2 catalyst:

DOI: 10.1021/acs.jpcc.7b04420
J. Phys. Chem. C 2017, 121, 14717−14724

Nature and role of different Au species. *J. Phys. Chem. C* **2009**, *113*, 3726−3734.
(35) Kresse, G.; Hafner, J. A. Ab initio molecular dynamics for liquid metals. *Phys. Rev. B: Condens. Matter Mater. Phys.* **1993**, *47*, 558.
(36) Kresse, G.; Hafner, J. A. Ab initio molecular-dynamics simulation of the liquid-metal-amorphous-semiconductor transition in germanium. *Phys. Rev. B: Condens. Matter Mater. Phys.* **1994**, *49*, 14251−14269.
(37) Kresse, G.; Furthmüller, J. Efficiency of ab-initio total energy calculations for metals and semiconductors using a plane-wave basis set. *Comput. Mater. Sci.* **1996**, *6*, 15.
(38) Kresse, G.; Furthmüller, J. Efficient iterative schemes for ab initio total-energy calculations using a plane-wave basis set. *Phys. Rev. B: Condens. Matter Mater. Phys.* **1996**, *54*, 11169.
(39) Perdew, J. P.; Burke, K.; Ernzerhof, M. Generalized gradient approximation made simple. *Phys. Rev. Lett.* **1996**, *77*, 3865.
(40) Perdew, J. P.; Burke, K.; Ernzerhof, M. Erratum: Generalized gradient approximation made simple. *Phys. Rev. Lett.* **1997**, *78*, 1396.
(41) Blöchl, P. E. Projector augmented-wave method. *Phys. Rev. B: Condens. Matter Mater. Phys.* **1994**, *50*, 17953.
(42) Kresse, G.; Joubert, J. From ultrasoft pseudopotentials to the projector augmented-wave method. *Phys. Rev. B: Condens. Matter Mater. Phys.* **1999**, *59*, 1758.
(43) Davidson, E. *Methods in Computational Molecular Physics*; Plenum: New York, 1983.
(44) Liu, B. In *Report on the Workshop: Numerical Algorithms in Chemistry: Algebraic Methods*; Moler, C., Shavitt, I., Eds.; Lawrence Berkeley Laboratory, University of California: Berkley, CA, 1978.
(45) Schlexer, P.; Pacchioni, G. Modelling of an ultra-thin silicatene/silicon-carbide hybrid film. *J. Phys.: Condens. Matter* **2016**, *28*, 364005.
(46) Monkhorst, H. J.; Pack, J. D. Special points for Brillouin-zone integrations. *Phys. Rev. B* **1976**, *13*, 5188.
(47) Stoneham, A. M. Systematics of metal-insulator interfacial energies: A new rule for wetting and strong catalyst-support interactions. *Appl. Surf. Sci.* **1983**, *14*, 249−259.
(48) Ruiz Puigdollers, A.; Schlexer, P.; Pacchioni, G. Gold and silver clusters on TiO_2 and ZrO_2 (101) surfaces: role of dispersion forces. *J. Phys. Chem. C* **2015**, *119*, 15381.
(49) Grimme, S. Semiempirical GGA-type density functional constructed with a long-range dispersion correction. *J. Comput. Chem.* **2006**, *27*, 1787.
(50) Tosoni, S.; Sauer, J. Accurate quantum chemical energies for the interaction of hydrocarbons with oxide surfaces: CH_4/MgO (001). *Phys. Chem. Chem. Phys.* **2010**, *12*, 14330−14340.
(51) Dion, M.; Rydberg, H.; Schroder, E.; Langreth, D. C.; Lundqvist, B. I. Van der Waals density functional for general geometries. *Phys. Rev. Lett.* **2004**, *92*, 246401.
(52) Chen, H. Y. T.; Pacchioni, G. Properties of two-dimensional insulators: a DFT study of Co adsorption on NaCl and MgO ultrathin films. *Phys. Chem. Chem. Phys.* **2014**, *16*, 21838−21845.
(53) Puigdollers, A. R.; Schlexer, P.; Pacchioni, G. Gold and silver clusters on TiO_2 and ZrO_2 (101) surfaces: role of dispersion forces. *J. Phys. Chem. C* **2015**, *119*, 15381−15389.
(54) Tang, W.; Sanville, E.; Henkelman, G. A grid-based Bader analysis algorithm without lattice bias. *J. Phys.: Condens. Matter* **2009**, *21*, 084204.
(55) Sanville, E.; Kenny, S. D.; Smith, R.; Henkelman, G. Improved grid-based algorithm for Bader charge allocation. *J. Comput. Chem.* **2007**, *28*, 899−908.
(56) Henkelman, G.; Arnaldsson, A.; Jonsson, H. A fast and robust algorithm for Bader decomposition of charge density. *Comput. Mater. Sci.* **2006**, *36*, 354.
(57) Vayssilov, G. N.; Gates, B. C.; Rösch, N. Oxidation of supported rhodium clusters by support hydroxy groups. *Angew. Chem., Int. Ed.* **2003**, *42*, 1391−1394.
(58) Ivanova Shor, E. A.; Nasluzov, V. A.; Shor, A. M.; Vayssilov, G. N.; Rösch, N. J. Reverse Hydrogen Spillover onto Zeolite-Supported Metal Clusters: An Embedded Cluster Density Functional Study of Models M_6 (M = Rh, Ir, or Au). *J. Phys. Chem. C* **2007**, *111*, 12340−12351.
(59) Hu, C. H.; Chizallet, C.; Mager-Maury, C.; Corral-Valero, M.; Sautet, P.; Toulhoat, H.; Raybaud, P. Modulation of catalyst particle structure upon support hydroxylation: ab initio insights into Pd_{13} and Pt_{13}/γ-Al_2O_3. *J. Catal.* **2010**, *274*, 99−110.
(60) Mager-Maury, C.; Chizallet, C.; Sautet, P.; Raybaud, P. Platinum nanoclusters stabilized on γ-Alumina by chlorine used as a capping surface ligand: a density functional theory study. *ACS Catal.* **2012**, *2*, 1346−1357.
(61) Wendt, S.; Kim, Y. D.; Goodman, D. W. Identification of defect sites on oxide surfaces by metastable impact electron spectroscopy. *Prog. Surf. Sci.* **2003**, *74*, 141.
(62) Kim, Y. D.; Wei, T.; Goodman, D. W. Identification of defect sites on SiO_2 thin films grown on Mo(112). *Langmuir* **2003**, *19*, 354.
(63) Wallace, W. T.; Min, B. K.; Goodman, D. W. The nucleation, growth, and stability of oxide-supported metal clusters. *Top. Catal.* **2005**, *34*, 17.
(64) Lopez, N.; Illas, F.; Pacchioni, G. Ab initio theory of metal deposition on SiO_2. I. Cu_n (n = 1−5) clusters on non-bridging oxygen defects. *J. Phys. Chem. B* **1999**, *103*, 1712−1718.

DOI: 10.1021/acs.jpcc.7b04420
J. Phys. Chem. C 2017, 121, 14717−14724